

Project: 1034

Project title: JPI-Climate project InterDec

Project lead: Dr. Daniela Matei

PIs: Dr. Daniela Matei, Dr. Jürgen Bader, Dr. Katja Lohmann, Dr. Elisa Manzini.

Allocated period: **2019-01-01 to 2019-12-31**

Abstract

InterDec-MPI aims at understanding the origin of decadal-scale climate variability in different regions of the world and the linkages between them by using observational data sets and through coordinated multi-model experiments. How can a decadal-scale climate anomaly in one region influence very distant areas of the planet? This can happen through atmospheric or oceanic teleconnections. Fast signal communication between different latitudinal belts within days or weeks is possible through atmospheric teleconnection, whereas communication through oceanic pathways is much slower requiring years to decades or even longer. Understanding these processes will enhance decadal climate prediction of both mean climate variations and associated trends in regional extreme events.

Achievements in 2019:

Ural blocking driving extreme Arctic sea-ice loss, cold Eurasia and stratospheric vortex weakening in autumn and early winter 2016-2017

We investigated the dynamics that led to the repeated cold spells over mid-latitude Eurasia, exceptionally warm conditions and sea-ice deficit over the Arctic, as well as the significant weakening of the stratospheric polar vortex in autumn and early winter 2016-2017 (Tyrlis et al., 2019). To this aim we used ERA-Interim reanalysis data, as well as COBE sea-ice and SST observational data with view to trace the pathways that led to these extreme conditions. Abundant blocking activity was observed over Eurasia during autumn (Fig. 1ab). Specifically over the Ural sector, the highest blocking activity throughout the ERA-Interim period was observed in autumn 2016 featuring a four-fold increase compared to climatological levels (Fig. 1c). In early autumn the sea-ice deficit was found over the Beaufort and East Siberian Seas but in November and December 2016 the deficit grew to unprecedented levels over the BKS (Fig. 1d).

Successive Ural blocking episodes (labeled B1-B4 in Fig. 2d) contributed to the sea-ice deficit observed in late autumn over the Barents-Kara Seas (BKS). Each episode induced circulation anomalies that resulted in cold air advection to the south and warm advection to the north of the blocking ridge. Repeated cold spells occurred over Central Asia while intrusions of warm and moist air resulted in enhancement of the sea-ice anomalies over the Barents-Kara Seas (BKS) featuring large concurrent variability on synoptic timescales whose pace was controlled by Ural Blocking (UB) activity (Fig.2ab). Actually, the BKS sea-ice cover minimum for 2016 was recorded in mid-November and December (labeled C1 and C2 in Fig. 2b) after the two Ural blocking episodes B3 and B4. Thus, the sea-ice deficit over the BKS in late autumn 2016 was mostly a consequence of the circulation induced by blocking.

A significant weakening of the stratospheric polar vortex was observed in late autumn 2016. The stratospheric vortex weakening is evident when exploring the evolution of the Polar Cap Height Index (PCHI) timeseries at 10 hPa (orange line in Fig. 2c). The PCHI corresponds to geopotential height area-averaged to the north of 65°N. Several peaks in the PCHI can be identified around the dates 31 October, 8, 15 and 25 November 2016 (labeled S1-S4) corresponding to episodes of stratospheric vortex weakening. The ones in early and late November (S1 and S4) represent the highest November PCHI values observed throughout the ERA-Interim period. These episodes of stratospheric vortex weakening encompass at least other two episodes in mid-November (S2 and S3). This stratospheric anomaly is unprecedented for November but is typical for late winter when sudden stratospheric events usually occur.

Each individual Ural blocking episode induced enhanced meridional displacements of air masses, arctic intrusions to its east and poleward intrusions to its west resulting to maxima of poleward eddy heat flux in the vicinity of the blocking. Thus, each blocking episode drove intense upward propagation of wave activity flux $F(p)$ (Fig. 2d) that resulted in episodes of stratospheric vortex weakening. On average, the peaks of $F(p)$ lagged the ones of Ural blocking episodes by around 10 days. Both major episodes of stratospheric vortex weakening S1 and S4 can be directly attributed to easterly tendency arising from divergence of the vertical component of the EP flux ($U_{\text{tend}}\text{DEPF}$, blue line in Fig. 2c), following blocking episodes B2 and B3.

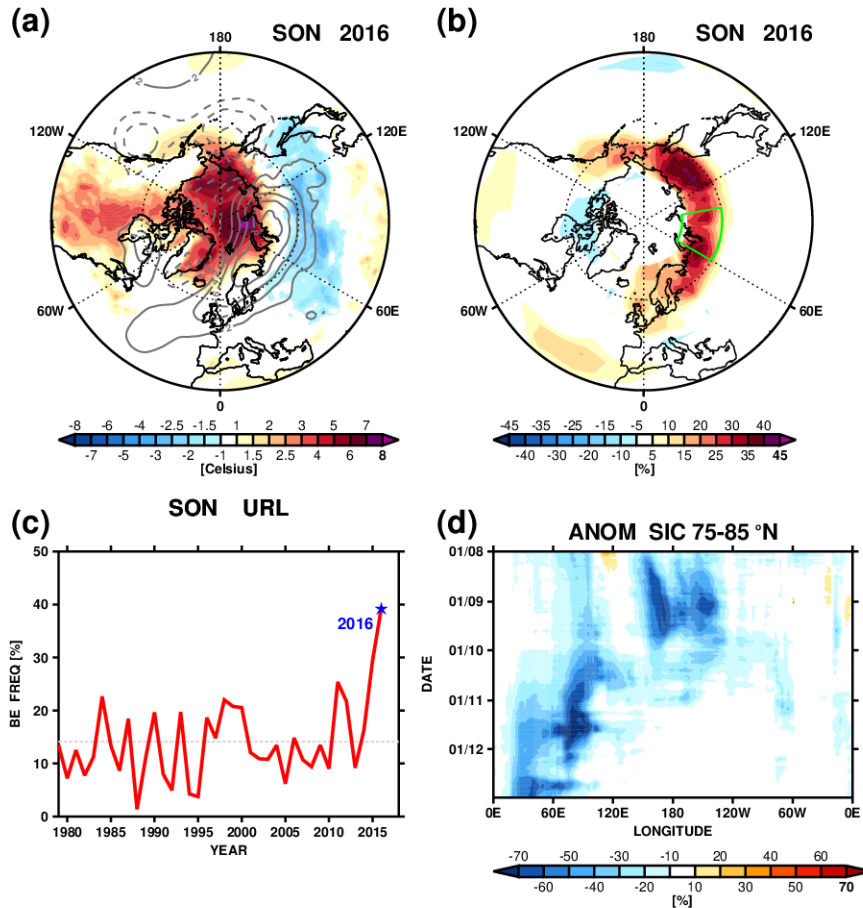


Figure 1. (a) Anomalous SON-mean MSLP (contours, hPa) and T2m (shades, Kelvin) for SON 2016. (b) Anomalous blocking episode frequency for SON 2016. (c) Interannual evolution of blocking episode frequency (%) averaged over the Ural sector that is delineated in (b). Dashed horizontal line shows the climatological value of Ural blocking episode occurrence. (d) Hovmöller diagram showing the evolution of daily Sea Ice Cover (SIC, in %) anomalies within the latitude band 75-85°N during the period August-December 2016. (from Tyrllis et al., 2019)

Overall, UB had a key role in linking the significant circulation anomalies observed in the Troposphere, Stratosphere, as well as Arctic sea-ice loss in autumn 2016. The study of changes in blocking frequency, intensity and location can be a useful tool to study the impact of changes in the Arctic Cryosphere to the mid-latitude circulation as well as feedbacks.

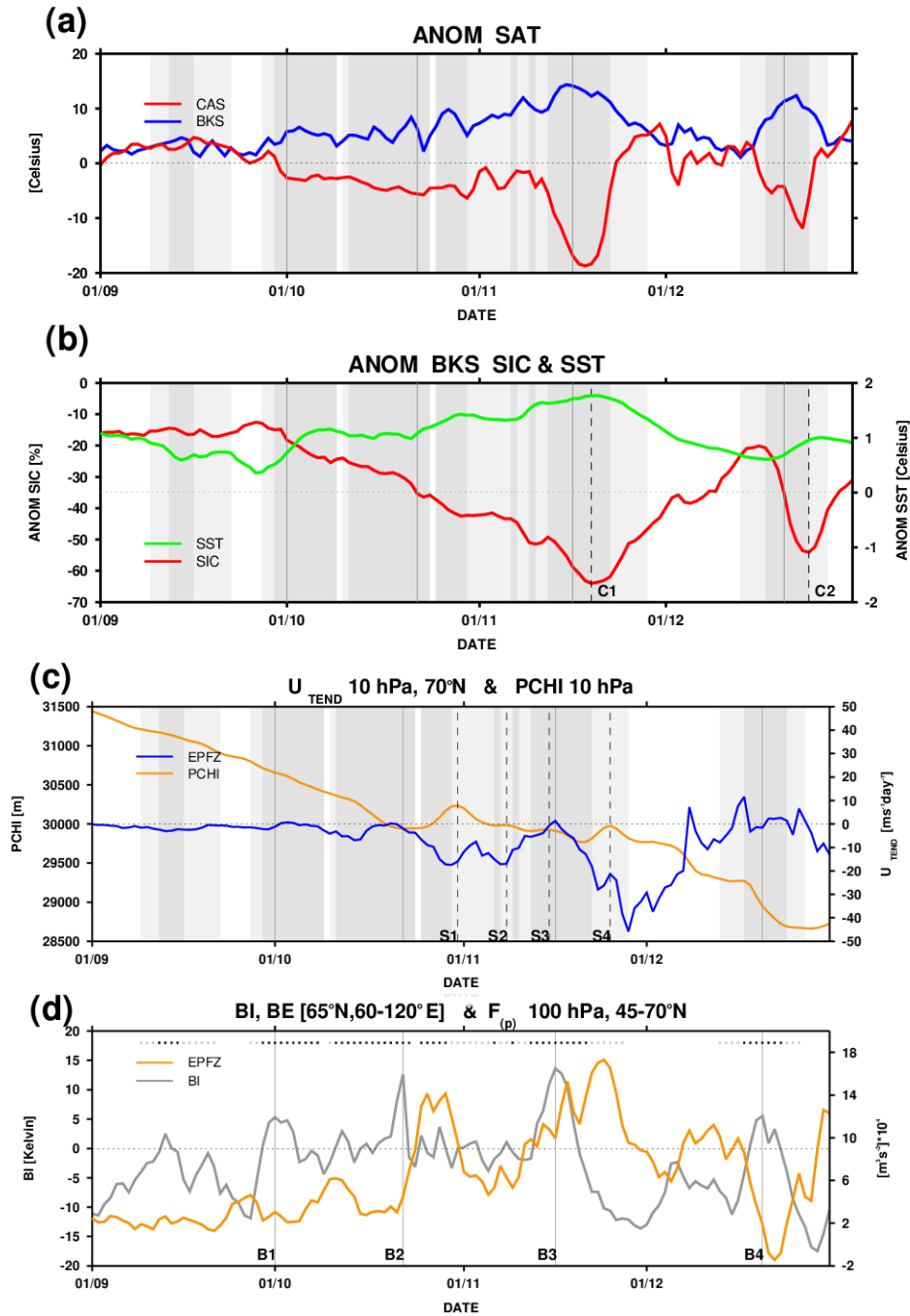


Figure 2. (a) Area-averaged SAT anomalies over the BKS (blue) and Central Asia (CAS, red). (b) Area-averaged SST (green) and COBE SIC (red) anomalies over the BKS. Dashed vertical lines mark the dates of maximum SIC deficit (C1-C2). (c) Evolution of daily mean values of zonal wind tendency due to divergence of the vertical component of Eliassen- Palm flux $U_{TEND}DEPF_z$ (blue) and PCHI at 10 hPa (orange). Tendency is shown in units of $ms^{-1}day^{-1}$. Negative values indicate periods of easterly tendency that results in a weakening of the intensity of the polar vortex. Dashed vertical lines mark the dates of episodes of weakening of the stratospheric polar vortex (S1-S4). (d) Evolution of the Blocking Index (BI in Kelvin, grey) averaged over the Ural sector (65°N, 60-120°E) and the vertical component of the Eliassen-Palm flux $F_{(p)}$ at 100 hPa, which is averaged within the latitudinal band 45-70°N (orange in $m^3s^{-2}*10^4$). Light (heavy) grey dots or areas mark dates when BE is identified in at least one grid-point (in more than 50% of grid-points) within the Ural sector. Solid vertical lines mark the dates of the four major blocking episodes (B1-B4). The data spans the period 1 September - 31 December 2016. (from Tyrlis et al., 2019)

Coordinated Arctic sea-ice sensitivity experiments

The InterDec coordinated Arctic sea-ice sensitivity experiments have been carried out by four global modelling centers (Table1). The protocol of the coordinated experiments asks for the inter-comparison of three simulations, each 110-year long (first 10 years considered to be the spin up period). Each simulation is carried out with an atmosphere general circulation model forced by climatological sea surface temperature (SST) and sea ice concentrations (SIC). While the climatological SSTs are the same for the three simulations, the SICs are defined so as to represent low sea ice, climatological, and high sea ice conditions, respectively denoted LICE, CLIM, and HICE. The SST and SIC forcing dataset (the COBE dataset) has been provided by the University of Niigata (partner of InterDec). The COBE dataset was chosen, because (1) the data are available in daily resolution and (2) the SICs and SSTs are adjusted in a physically consistent way. The climatological average of the SST and SIC covers time period July 1981 to June 2016. The LICE or HICE SICs are averages over the 10 years in which the observational November SICs over the Barents-Kara Sea (BKS) are lowest or highest (respectively), considering the time period July 1981 to June 2016. Hereafter we present preliminary results of the LICE and HICE inter-comparison, across the four InterDec models. The aim is to examine influences of the recent Arctic sea ice loss on tropospheric and stratospheric circulations based on multiple high-top AGCM experiments (all the InterDec models are high top models, Gerber et al 2012).

Table 1. Atmospheric Models participating in the InterDec Coordinated Experiments

Model	Developed at	Resolution	Model top	QBO
ECHAM6	MPI	T63L47	80km	No
AFES4.1	JAMSTEC	T79L56	60km	No
SC-WACCM	NCAR	1.9x2.5 ^o , L66	150km	Yes
IFS	ECMWF, SMHI	T255L91	80km	Yes

In the following, the response of the atmosphere to sea ice loss is shown by means of the LICE minus HICE difference in December to February (DJF) 100-yr mean for near surface air temperature (Figure 3, four panels at left), pressure at sea level (PSL, Figure 3, four panels at right) and in daily zonal mean zonal wind at 60°N, from the beginning of November to the end of March, 100-yr mean (Figure 4).

All models show comparable and significant warming over the BKS region, indicating that the forcing is consistent across the models (Figure 3, four panels at left). However, especially over the Eurasian continent, the near surface temperature response differs across the models. The response for the ECHAM and WACCM is significant over Asia, but of opposite sign. The response in the remaining two models is very weak. The across model differences in near surface temperature response are of dynamical origin, as demonstrated by the PSL response (Figure 1, four panels at right). A prominent Siberian high-pressure response is realized only for the ECHAM model, explaining the cooling over the Asia region for that model. Three models show consistently a low-pressure response over Europe. For the IFS model, the pattern of the response is rather annular.

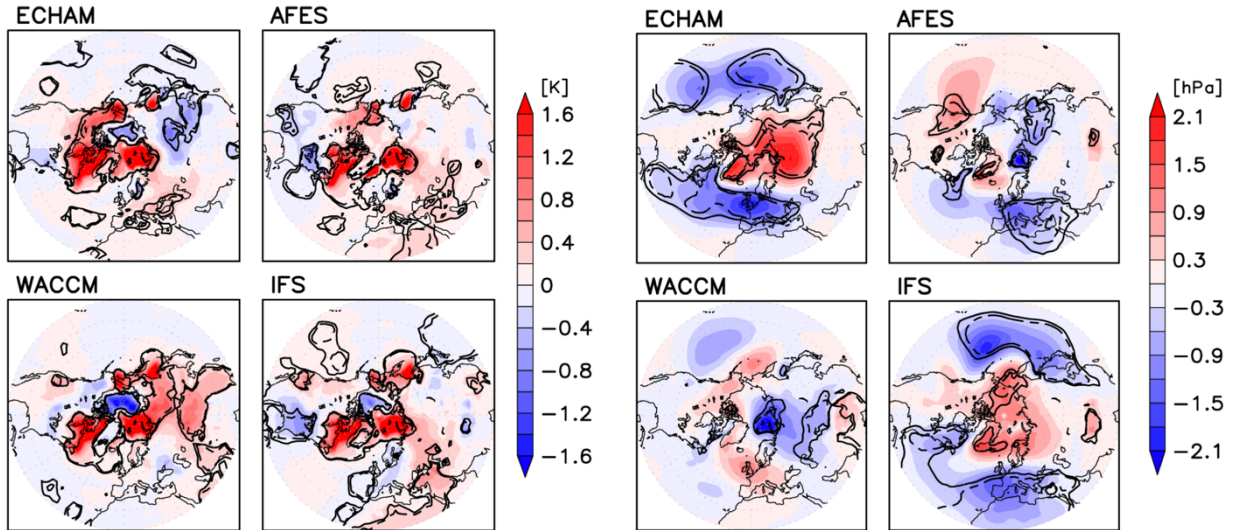


Figure 3. LICE minus HICE difference in December to February (DJF) 100-yr mean for near surface air temperature (four panels at left) and for pressure at sea level (four panels at right); respectively, clockwise, for the ECHAM, AFES, IFS and WACCM models. Contours depict statistical significance at 90 and 95% levels. (Hoshi et al., in preparation)

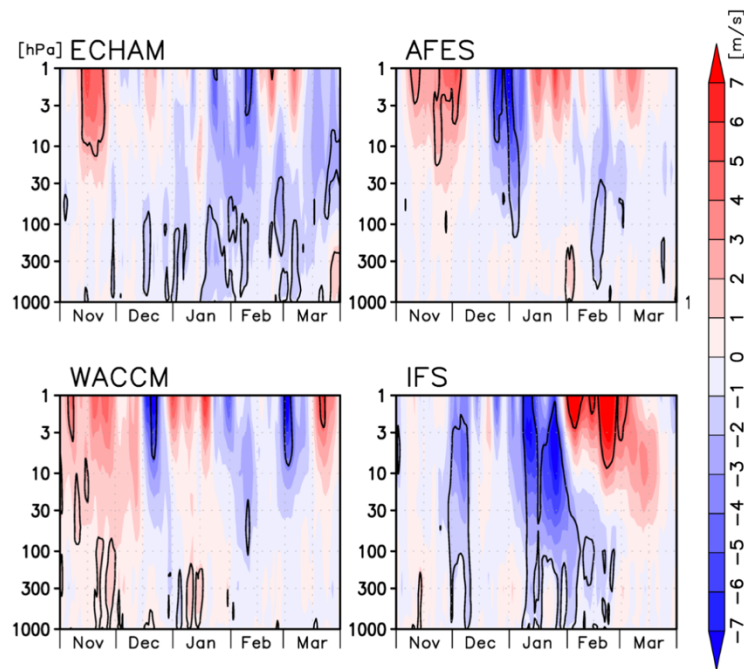


Figure 4. LICE minus HICE difference in 100-yr mean of daily zonal mean zonal wind at 60°N from the beginning of November to the end of March. Contours depict statistical significance at 90% level. (Hoshi et al., in preparation)

To evaluate the involvement of the stratospheric pathway in the near surface dynamical response to sea ice loss (Hoshi et al 2017), we next look at the daily evolution of the 100-yr mean in zonal mean zonal wind at 60°N (Figure 4). A clear involvement is evident for the IFS model, so explaining the near-annular response in PSL for that model. Throughout all the month of January the stratospheric

polar vortex weakens for the IFS model. The January vortex weakening therefore can contribute the tropospheric wind response and the near surface dynamical response by downward stratosphere to troposphere coupling, during February. The stratospheric polar vortex tends to weaken also in the remaining three models. However, for two models (AFES and WACCM) the duration of the vortex weakening in the lower stratosphere is not persistent, a plausible reason for a lack of downward coupling. In the case of the ECHAM model, there seems to be the signature of downward coupling in the zonal mean zonal wind, but very late in the season, specifically in March, mostly. The strong and significant DJF PSL and near surface responses of the ECHAM model are therefore attributed to the tropospheric link between sea ice loss and atmospheric circulation, involving tropospheric atmospheric blocking. Analysis of the atmospheric blocking occurrence by means of daily outputs to demonstrate this latter interpretation is ongoing.

References

Gerber, E. P., et al (2012) Assessing and understanding the impact of stratospheric dynamics and variability on the Earth system. *Bull. Am. Meteorol. Soc.* 93, 845-859. DOI 10.1175/BAMS-D-11-00145.1

Hoshi, K., et al (2017), Poleward eddy heat flux anomalies associated with recent Arctic sea ice loss, *Geophys. Res. Lett.*, 44, 446–454, doi:10.1002/2016GL071893

Tyrlis E., Manzini E., Bader J., Ukita J., Nakamura H. and Matei D. (2019): Ural blocking driving extreme Arctic sea-ice loss, cold Eurasia and stratospheric vortex weakening in autumn and early winter 2016-2017, *Journal of Geophysical Research – Atmospheres*, doi: 10.1029/2019JD031085